J Mater Sci (2006) 41:6193–6197
DOI 10.1007/s10853-006-0361-8

INTERFACE SCIENCE

Temperature dependence of fractal dimension of grain boundary region in SnO_2 based ceramics

Goran Branković · Zorica Branković · Daniela Russo Leite · José Arana Varela

Published online: 29 June 2006

Abstract Fractal dimensions of grain boundary region in doped SnO_2 ceramics were determined based on previously derived fractal model. This model considers fractal dimension as a measure of homogeneity of distribution of charge carriers. Application of the derived fractal model enables calculation of fractal dimension using results of impedance spectroscopy. The model was verified by experimentally determined temperature dependence of the fractal dimension of SnO_2 ceramics. Obtained results confirm that the non-Debye response of the grain boundary region is connected with distribution of defects and consequently with a homogeneity of a distribution of the charge carriers. Also, it was found that C–T^{-1} function has maximum at temperature at which the change in dominant type of defects takes place. This effect could be considered as a third-order transition.

Introduction

Impedance spectroscopy (IS) analysis of ceramic materials enables separation of bulk and boundary components of the conductivity [1, 2]. In an ideal case, the result of IS measurements over a wide range of frequencies can be presented by several semicircles in the complex Z_{Re}–Z_{Im} plane (Nyquist plot) [2, 3]. Measured values in the form of Nyquist plots are rarely ideal semicircles. Most of the authors describe them as depressed and/or deformed semicircles, with the center lying below the x-axis. This phenomenon, called non-Debye relaxation [4, 5], is attributed to the distribution of Debye relaxation with different time constants [6]. There are several papers in the literature [1, 7–9] treating this phenomenon very systematically.

Depressed semicircle in impedance spectra could be presented by equivalent circuit containing CPE (constant phase element). In literature already exist some models that consider existence of CPE in equivalent circuit of rough surfaces using fractal theory [10–12]. However, these models couldn't explain temperature dependence of fractal dimension.

Recently, we proposed a novel fractal model to explain non-Debye response in ceramics materials with highly resistive grain boundaries [13]. This model gives a physical explanation of parameter β from the Davidson–Cole equation (Eq. 1).

$$Z = Z_{Re} + j \cdot Z_{Im} = R_G + \frac{R_{GB}}{(1 + j\omega R_{GB} C)^{\beta}} \quad (1)$$

where Z is the overall impedance, Z_{Re} and Z_{Im} are the real and imaginary components of the impedance, R_G is the resistance of the grains interior, R_{GB} is the resistance of the grain boundary region, β is a constant, while C represents the capacitance of the grain boundary region.

It has to be pointed out that this model considers a region inside the grains, close to the grain boundaries, with laterally inhomogeneous distribution of defects and dopants and consequently inhomogeneous distribution of charge carriers. Inhomogeneous distribution of the charge carriers in the vicinity of grain boundaries results in local

G. Branković (✉) · Z. Branković
Center for Multidisciplinary, Studies of University of Belgrade, Kneza Višeslava 1a, 11030 Belgrade, Serbia & Montenegro
e-mail: brankog@ibiss.bg.ac.yu

D. R. Leite · J. A. Varela
Instituto de Quimica, UNESP, P.O. Box 355, CEP: 14.801-970 Araraquara, SP, Brasil

fluctuations in the resistance of this region. These effects lead to a non-ideal response of the grain boundary region. Based on these assumptions the fractal model was constructed and the equation that connects the fractal dimension with the parameter β from the Davidson–Cole equation was derived.

Observation and determination of lateral distribution of the charge carriers in the vicinity of one-grain boundary is almost impossible using microscopic techniques, such as SEM, TEM or even HRTEM. On the other hand J. R. Macdonald stated that a model that treats non-Debye relaxation in ceramics could be valid only if it enables explanation of temperature dependence of depression angle [14]. Because of that in this work the fractal model was verified by experimentally determined temperature dependence of the fractal dimension of doped SnO_2 ceramics which is typical example of electroceramics with highly resistive grain boundaries.

Experimental procedure

SnO_2 samples containing small quantities of CoO were prepared by the method of evaporation and decomposition of solutions and suspensions. Starting materials were: SnO_2 and $Co(CH_3COO)_2$. Samples were prepared by the following procedure:

Appropriate amount of $Co(CH_3COO)_2$ was dissolved in 25 ml of water to obtain solution according to desired composition of final powder mixture. Further, 5 g SnO_2 powder (surface area = 6 m^2/g) was suspended in solution of $Co(CH_3COO)_2$. Suspension was stirred and heated on the hot magnetic plate and dried at 410 K for 5 h. Obtained powder mixture was milled in agate mortar and calcined at 1373 K. After thermal treatment the obtained powder had the compositions of 99 mol. % SnO_2 + 1 mol. % CoO.

Powders of undoped SnO_2 and CoO doped SnO_2 were isostatically pressed at 250 MPa in pellets sized approximately 1 mm in height and 8 mm in diameter and sintered in synthetic air (mixture of O_2 and N_2) at 1623 K for 2 h (compositions with Co^{2+}), and 1823 K for 8 h (undoped SnO_2). Sintered samples were characterized by ac impedance spectroscopy (HP 4192A) in frequency range from 100 Hz to 1 MHz, using Au sputtered electrodes. Measurements were performed in air or N_2 atmosphere.

Results and discussion

Fractal model

It is necessary to briefly present the main features of the derived fractal model for better understanding of the experimental results. It is assumed that there is no homogeneous spatial distribution of defects and dopants in the vicinity of grain boundaries. These effects result in laterally inhomogeneous distribution of charge carriers and are supposed to be the main reason for the non-Debye behaviour of the grain boundaries. It is also assumed that the grain boundary is a smooth plane, but there are differences in distribution of defects in the vicinity of the grain boundary which result in different resistances across the grain boundary region (Fig. 1a). If the region in the vicinity of the grain boundary is observed with one resolution, it could be represented by boxes with different heights, where the height of the box is proportional to the resistance (Fig. 1b). Hence, boxes with larger resistance are higher and vice versa. The associated capacitance is proportional to the area (S) of the surface normal to the electrical field direction. This surface also has its own resistance, proportional to S^{-1} named as the interface resistance. If the resolution is increased it will be possible to recognize non-uniformity within each box, so that each box could be divided into new boxes with uniform resistance and capacitance, and so on. It was also assumed that the observed region could be treated as a fractal object. A region in the vicinity of the grain boundary, shown in Fig. 1b, could be divided into M parts (not necessarily of the same shape) with the same surface area and the same concentration of charge carriers. An example of such a part is shown in Fig. 1c. Magnification of this picture by factor a (scaling factor) will show that each part has local inhomogeneities, i.e., there are N randomly distributed boxes with a higher resistance within each part. Resistance R_B is the resistance of the whole part up to $z = h$. Capacitance of that surface ($z = h$) is C and the interface resistance is R_I. The resistance of each of the N boxes has the value $R_{B1} = a \cdot R_B$, capacitance has the value $C_1 = C/a^2$, and interface resistance is $R_{I1} = R_I \cdot a^2$. Further magnification by a reveals a new layer with $R_{B2} = a^2 \cdot R_{B1}$, $C_2 = C/a4$, and $R_{I2} = R_I \cdot a^4$ etc. The impedance of a whole region in the vicinity of the grain boundary is $Z_{tot} = Z(\omega)/M$, where $Z(\omega)$ represents the impedance of the part shown in Fig. 1c. The equivalent circuit for such part is given in Fig. 2 and can be described by the following equation

$$Z(\omega) = R_B + \cfrac{1}{\cfrac{1+j\omega R_I C}{R_I} + \cfrac{N}{R_B \cdot a + \cfrac{1}{\cfrac{1+j\omega R_I C}{R_I a^2} + \cfrac{N}{R_B \cdot a^2 + \cfrac{1}{\cfrac{1+j\omega R_I C}{R_I a^4} + \cfrac{N}{R_B \cdot a^3 + \cfrac{1}{\cfrac{1+j\omega R_I C}{R_I a^6} + \ldots}}}}}}} \quad (2)$$

Using a simple mathematical procedure it is possible to simplify and solve this equation. A solution of the Eq. (2) is in the form of the Davidson–Cole equation, where K is

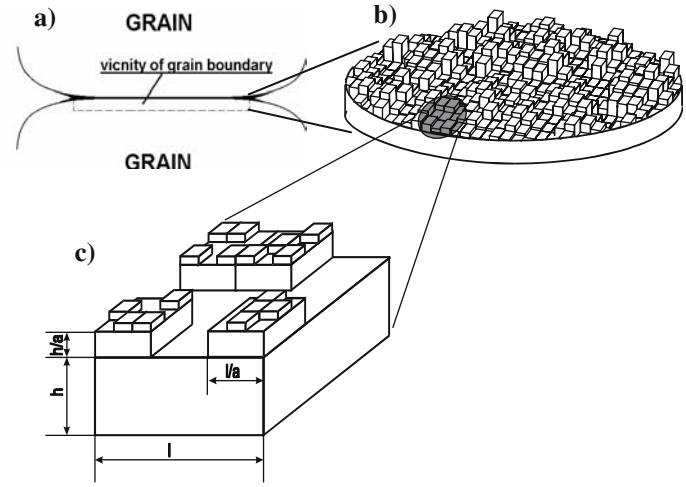

Fig. 1 (**a**) Region in the vicinity of grain boundaries considered by fractal model, (**b**) inhomogeneous distribution of defects in the vicinity of the grain boundary resulting in different resistance (parts with different resistance are shown as boxes of different heights), (**c**) one part of grain boundary with self-similar properties

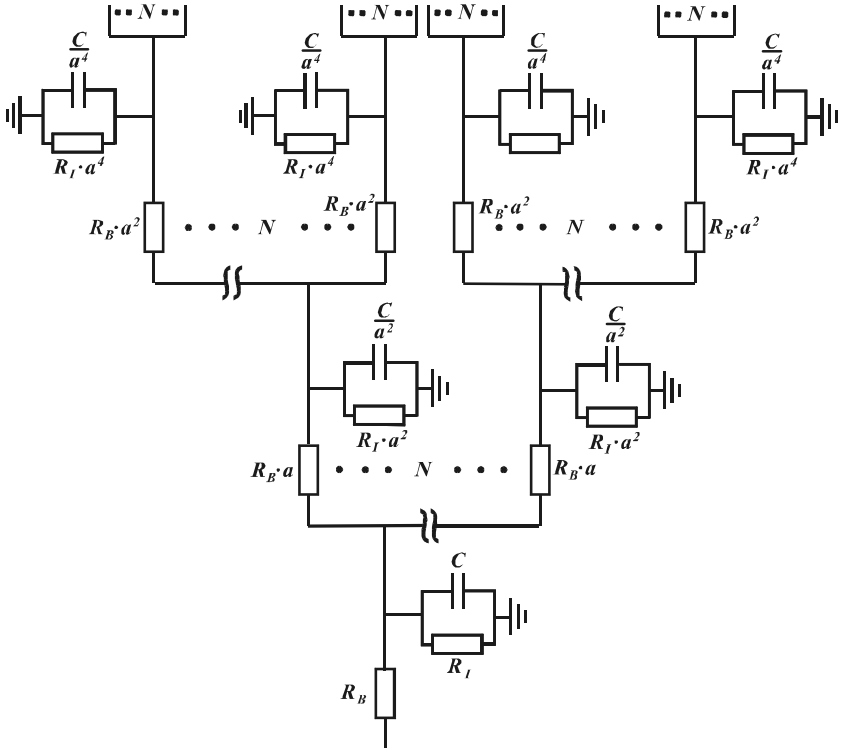

Fig. 2 The equivalent circuit of the model shown in Fig. 1c

constant, and other symbols have the earlier defined meanings.

$$Z(\Omega) = K\Omega^{-\beta} = K\left(\frac{1 + j\omega R_1 C}{R_1}\right)^{-\beta} \quad (3)$$

Considering the definition of the deterministic fractal dimension as $d_s = \ln N / \ln a$ it is possible to get final equation which connects the fractal dimension (d_s) with parameter β:

$$d_S = 1 + \beta. \quad (4)$$

The complete derivation procedure was given in the Ref. 13. This fractal dimension is related to the inhomogeneous distribution of charge carriers in the vicinity of the grain boundary surface.

Fractal dimension of the doped SnO_2

Using the results of fitting of IS (Fig. 3) with Davidson–Cole equation and Eq. (4) the values of fractal dimension (d_S), resistance (R) and capacitance per unit area of a grain boundary (C) were determined based on brick-layer model.

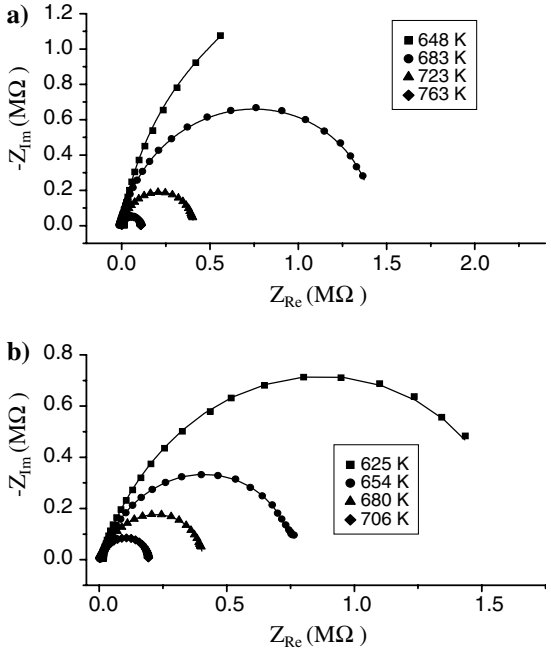

Fig. 3 AC impedance spectroscopy spectra of samples: (**a**) pure SnO_2, and (**b**) SnO_2 + 1% CoO measured in N_2

Obtained values of capacitances are characteristic for grain boundary regions [15]. Changes of d_S, C and ln$R$ as the functions of temperature of the samples are given in Fig. 4. All samples show same behaviour: Curves C–T^{-1} and ds–T^{-1} have extreme values at the same temperature as the temperature at which function ln$R$–T^{-1} have change in slope. Change in slope of function ln$R$–T^{-1} is consequence of change in dominant type of defects. For example, in sample doped with 1% of Co^{2+}(measured in N_2) one type of defects (energy level) is dominant for temperatures lower than 680 K, i.e. at temperatures lower than 680 K the ionization of one type of defects is dominant. For temperatures around 680 K there is high influence of other defect level, which start to be the dominant one after 680 K. Fractal dimension shows minimal value around 680 K, i.e. at temperature at which is the highest disorder of the system. Further increase in temperature results in ionization of another type of defects and a second type of energy level is dominant, so the fractal dimension increases. This means that in this temperature interval the homogeneity of the charge carriers increases.

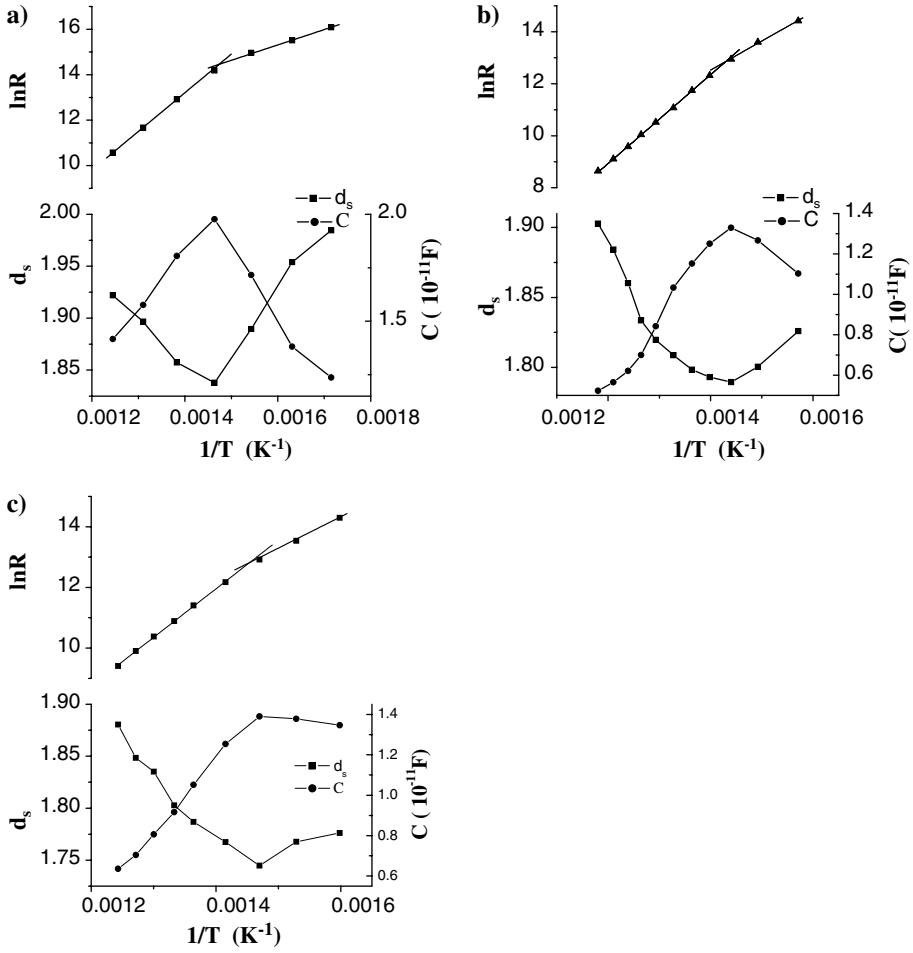

Fig. 4 Fractal dimension, capacitance and ln$R$ as a function of temperature of SnO_2 samples: (**a**) pure SnO_2, (**b**) SnO_2 + 1% CoO measured in air, (**c**) SnO_2 + 1% CoO measured in N_2

If we assume that the polarization P is proportional to local electric field E [16],

$$\vec{P} = \varepsilon_0(\varepsilon_r - 1)\vec{E}, \quad (5)$$

and that the classical Gibbs free energy (G) can be written as:

$$G = H - TS - \vec{P}\vec{E}, \quad (6)$$

then the second partial derivative of G related to E is:

$$\frac{\partial^2 G}{\partial E^2} = 2\varepsilon_0(\varepsilon_r - 1), \quad (7)$$

i.e. the second derivative of Gibbs energy ($\frac{\partial^2 G}{\partial E^2}$) is linear function of ϵ_r. Since different ionized defects have different dipole moments then function $\frac{\partial \varepsilon_r}{\partial T} \propto \frac{\partial^3 G}{\partial E^2 \partial T}$ has discontinuity at 680 K, indicating the existence of third-order transition.

Comparison of the functions given at Fig. 4 b and c, showed that the lower values of d_s are obtained in atmosphere of N_2. Bearing in mind that sintering was performed in air and that consequently defect equilibrium was achieved in air, it is logical that measurements in N_2 will change defect concentrations, especially at the grain boundaries closer to the open pores. This inhomogeneous change in defect concentrations will introduce more disorder into the system.

Obviously, it is possible to explain temperature dependence of the fractal dimension, i.e. parameter β from the Davidson–Cole equation, using the fractal model of the grain boundary region of ceramics. The fractal dimension and other electrical parameters of the grain boundary, such as resistance and capacitance, are connected to distribution and concentration of charge carriers, which are on the other hand strongly dependent of temperature. Consequently it is easy to explain temperature dependence of these characteristic parameters as it was done in above given analysis.

Conclusions

The fractal dimensions of pure and CoO doped SnO_2 ceramics were calculated based on previously derived fractal model of the grain boundary region in ceramics materials. Comparative study of temperature dependence of the fractal dimension and temperature dependence of other electrical parameters (capacitance and resistance) confirmed connection of fractal dimension with homogeneity of distribution of charge carriers. It was found that introducing of d_s as characteristic parameter of grain boundaries, through the given fractal model, has real physical meaning. Also, it was found that ϵ_r–T function has maximum at the same temperature at which function d_s–T^{-1} have minimum and that is the temperature at which change in dominant type of defects takes place. This effect could be considered as a third-order transition.

Acknowledgments This work was financially supported by Fundação de Amparo à Pesquisa do Estado de São Paulo (FAPESP) and by the Ministry for Science and Environmental Protection of Republic of Serbia.

References

1. Smith A, Baumard JF, Abélard P, Denanot MF (1989) J Appl Phys 65:5119
2. Jiang SP, Love JG, Badwal SPS (1997) In: Nowotny J, Sorrell CC (eds) Key engineering materials, vol. 125–126, Electrical properties of oxide materials, Trans Tech Publications, Switzerland, p 81
3. Kirkpatrick KS, Mason TO, Balachandran U, Poeppel RB (1994) J Am Ceram Soc 77:1493
4. Sletson LS, Potter ME, Alim MA (1988) J Am Ceram Soc 71:909
5. Alim MA (1989) J Am Ceram Soc 72:28
6. Modine FA, Major RW, Choi S-I, Bergman LB, Silver MN (1989) In: Levinson LM (ed) Ceramic transactions, vol. 3, Advances in varistor technology, The American Ceramic Society, Westerville, OH, p 176
7. Raistrick ID (1987) In: Macdonald JR (ed) Impedance spectroscopy: emphasizing solid materials and systems, John Wiley & Sons, p 27
8. Lindsey CP, Patterson GD (1980) J Chem Phys 73:3348
9. Jonscher AK (1975) Phys Stat Sol (a) 32:665
10. Kaplan T, Gray LJ (1985) Phys Rev B 32:7360
11. Kaplan T, Gray LJ, Liu SH (1987) Phys Rev B 35:5379
12. Liu SH, (1985) Phys Rev Lett 55:529
13. Branković G, Branković Z, Jović V, Varela JA (2001) J Electroceramics 7:89
14. Macdonald JR (1987) Impedance spectroscopy: emphasizing solid materials and systems, John Wiley & Sons
15. Lee J, Hwang J-H, Mashek JJ, Mason TO, Miller AE, Siegel RW (1995) J Mater Res 10:2295
16. Strobl G, (2004) Condensed matter physics Springer-Verlag Berlin Heidelberg